XII National and III International

Conference on Engineering Thermodynamics

12CNIT-2022 - FULL PAPER

Estimation of the solar thermal power generation potential in Pamplona (northern Spain)

Ignacio García[1,2], Eduardo Prieto[1], José Luis Torres[1].

[1]Institute of Smart Cities (ISC), Department of Engineering, Public University of Navarre, Campus Arrosadía, 31006 Pamplona, Spain, email: ignacio.garcia@unavarra.es.

[2]Solar and Wind Feasibility Technologies Research Group (SWIFT), Electromechanical Engineering Department, University of Burgos, 09006 Burgos, Spain.

Keywords: *Solar map; urban solar thermal potential; energy transition*

TOPIC: RENEWABLE ENERGIES, ENVIRONMENTAL IMPACT AND CIRCULARITY

1. Abstract

In this work, an analysis of the potential of the city of Pamplona to produce solar thermal energy was carried out, according to the solar radiation received. As a result, for each residential, industrial, or service rooftop, information was provided on (1) the area available for thermal installation, (2) the solar thermal installation capacity and (3) the monthly and annual thermal energy generation potential. It was found that, if all suitable areas of the city are used, it would be possible to achieve an annual total solar thermal energy production of 1197.69 GWh. If solar energy supply and thermal demand were perfectly coupled over time, it would be possible to cover 99.1% of Pamplona's thermal energy demand.

2. Introduction

For the last century there has been a growing concentration of population in cities century. This tendency is expected to continue unless the necessary policy measures are taken. According to the United Nations report [1], in 2018, 1.7 billion people –23 per cent of the world's population– lived in a city with at least 1 million inhabitants. In 2030, a projected 28 per cent of people worldwide will be concentrated in cities with at least 1 million inhabitants. This increase in population has been associated with a consequent growth in energy consumption. Though, cities have great potential for energy production from renewable sources, especially from solar radiation. Precisely the transition towards an energy model based on renewable energies will contribute to the fight against climate change. This affirmation is supported by different international treaties and initiatives such as the Paris Agreement [2] or the European Green Deal [3]. For this reason, several countries have made it mandatory for buildings to have renewable energy installations. In Spain, for example, this directive is regulated by the Technical Building Code (CTE, by its acronym in Spanish).

The rise of photovoltaic technology is overshadowing the development of solar thermal, so it is necessary to analyze the opportunity to install one or the other technology, since both are competing for the same space. This analysis is especially influenced by the type of energy needs of the final consumer (electric or thermal) as well as its spatial and temporal distribution.

In this regard, geographic information systems (GIS) are essential for analyzing the availability and potential use of renewable energies in cities, given their distributed nature. In fact, for some

years now, solar maps of different cities have proliferated [4]–[6], *i.e.*, GIS-based tools that make it possible to know the potential of photovoltaic and thermal energy production at building level. Against this background, this paper presents an evaluation of the solar thermal potential of the city of Pamplona (Spain). This study has arisen from the need of the Municipal Energy Agency of the Pamplona City Council to evaluate the renewable resources of the city and to stimulate their use.

The paper is structured as follows: Section 3 details the used meteorological and geographical data, Section 4 describes the methodology followed for the evaluation of Pamplona's solar thermal resource. Section 5 presents and discusses the main results obtained and Section 6 is devoted to conclusions.

3. Data

3.1. Meteorological data

The meteorological data used were obtained from the station located in the property of the Higher Technical School of Agricultural Engineering and Biosciences of the Public University of Navarre (Pamplona, Spain) (42º47'32'' N, 1º37'49'' W, 433 m a.s.l.). The dataset was registered from January 2005 to September 2020 with an hourly frequency, containing the following variables: horizontal global irradiance, temperature, and relative humidity. Irradiance data were subjected to the quality control (QC) procedure of the Baseline Surface Radiation Network (BSRN) [7] which establishes three levels of QC: physical limits, extreme limits and consistency. In the case of temperature and relative humidity data, only a control of extreme limits was applied. A Typical Meteorological Year (TMY) was generated from this dataset, suitable for the estimation of the solar resource in the long term [8]. Specifically, the Typical Global radiation Year (TGY) proposed by the National Renewable Energy Laboratory (NREL) [1] was used in this work. Calculations carried out in this study involved the separate treatment of the two components of solar radiation (direct and diffuse), whose measurements were not available at the meteorological station considered. Therefore, the Dirint model [9] was used for the estimation of these components, as it shown a good performance for Pamplona in previous comparative studies [10], [11].

3.2. Geographical data

The geographic information employed consisted of a Digital Surface Model (DSM), obtained from a LiDAR flight performed in 2017, with a resolution of 2x2 meters. This information is available at the Spatial Data Infrastructure of Navarre (IDENA, for its acronym in Spanish). Although the geographical scope of this study is restricted to the municipality of Pamplona, it was necessary to use a larger DSM to consider the effect of distant obstacles (mainly mountains) on the incident radiation. The cadastral information of Pamplona was used to associate the estimations of radiation and thermal production obtained for each pixel of the DSM to the different buildings in the city. This information was obtained in vectorial format (*Shapefile*) through the download service of the Land Wealth and Property Tax Service of the Government of Navarre.

4. Methodology

4.1. Generation of the orientation and tilt models from the DSM

The calculation of the irradiance reaching each pixel, considering its inclination and orientation, requires the determination of these last two variables from the DSM. In this study, the models of

orientations and inclinations were determined by means of two algorithms provided by the Geospatial Data Abstraction Library (GDAL) and executed in QGIS software. Thus, two models were obtained, one containing the azimuth (γ_p) or orientation of each pixel and the other with its inclination (β_p).

4.2. Calculation of the visible horizon from each pixel of the DSM

The determination of the angular elevation of the visible horizon –or skyline– at a given location allows to consider the effect of surrounding obstacles (buildings, trees, mountains, etc.) on the two components of solar radiation. Therefore, it was calculated the elevation of the horizon visible from each pixel of the DSM. To reduce the computational effort, the procedure described below was followed:

- Calculation of the near horizon for each DSM pixel considering a 500m radius and a step angle of 1º.
- Calculation of the far horizon for each defined grid cell considering the full extent of the DSM and a step angle of 1º. For this purpose, the city was divided into a series of 500mx500m cells, and a single far horizon calculation was performed for each cell.
- Combination of both, the near and the far horizon for each pixel. For this purpose, the upper envelope of the two horizons is considered as shown in Fig. 1.

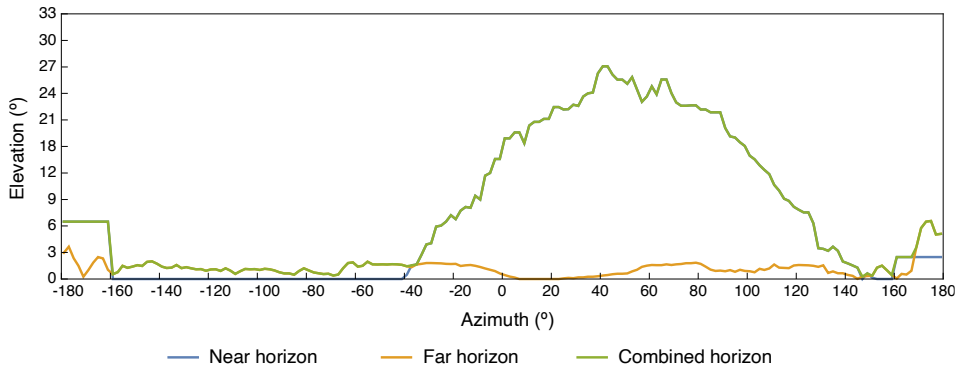

Figure 1. Profile of the horizon visible from a DSM pixel. The horizon line results from the combination of the far and near horizon lines.

4.3. Generation of the sky view factor map

The sky view factor (SVF) is the ratio of the diffuse irradiance received by a tilted plane to the horizontal diffuse irradiance considering an isotropic distribution of radiance in the sky. The role of this parameter in this study is twofold: on the one hand, it allows considering the effect of obstacles on the diffuse irradiance received at each pixel of the DSM. On the other hand, it is a parameter directly related to the definition of urban heat islands [12], [13]. When the plane is in an obstructed environment, the SVF corresponds to the quotient of Eq. (1).

$$SVF = \frac{G_{d,T,obs}}{G_d}, \tag{1}$$

where $G_{d,T,obs}$ is the diffuse irradiance received on a tilted plane considering the effect of obstacles and G_d is the diffuse irradiance received in a horizontal plane free of obstacles.

SVF estimation was carried out by means of Eq. (2) proposed by Böhner and Antonić [14] as an adaptation of the original expression of Dozier and Frew [15].

$$SVF = \frac{1}{N}\sum_{i=1}^{N} \max\left[0, \cos\beta_p \cos^2\alpha_i + \sin\beta_p \cos(\gamma_i - \gamma_p)\,(\pi/2 - \alpha_i - \sin\alpha_i \cos\alpha_i)\right], \quad (2)$$

where α_i is the angular elevation of the horizon corresponding to an azimuth γ_i, γ_p is the azimuth of the plane and N the total number of azimuths considered to define the horizon (360 in this case). Thus, for the calculation of the SVF at a pixel of the DSM, it is necessary to know its orientation, its tilt and the elevation of the visible horizon line (Section 4.2).

4.4. Calculation of the solar radiation map (global, direct, diffuse, and reflected radiation)

The conversion of the direct hourly irradiance on the horizontal plane to the tilted plane of each pixel follows a simple geometric relationship that considers the solar zenith angle and the angle of incidence between the sun and the pixel in question. The calculation of these two variables requires the prior determination of the position of the sun at each hour of the year. For this purpose, the updated algorithm of the Plataforma Solar de Almería (PSA) [16] was used. It is also necessary to consider the effect of environmental obstacles on the incident direct irradiance. That is, determining at each moment whether the obstacles are between the sun and the pixel or not. Fig. 2 shows the representation of the horizon elevation line corresponding to a given pixel and the solar analemmas corresponding to the position of the sun in the sky if it is observed every day of the year at the same times. When the sun is below the horizon it will not be visible, and the direct irradiance will be zero.

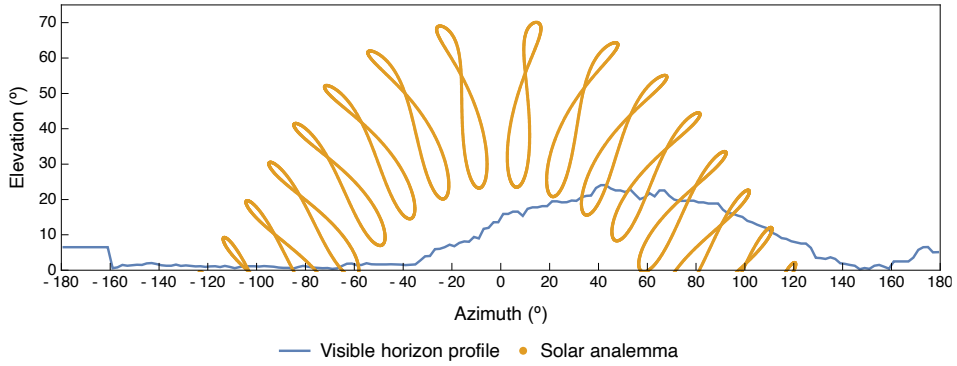

Figure 2. Horizon profile visible from a pixel of the DSM (blue line) and representation of the solar analemma for each UTC hour (yellow line).

Due to its multidirectional and anisotropic character, the calculation of the incident diffuse irradiance on a tilted plane cannot be solved with a simple geometric transformation, it is necessary to resort to a model. In this study, the model of Perez et al. [17] was used since it presents the best performance for Pamplona among the existing ones [18]. A modification of the original model was introduced to consider the effect of obstacles on the diffuse irradiance since the model, as it was conceived, only considered the effect of the inclination and orientation of the plane. A further contribution, corresponding to the diffuse irradiance reflected on the tilted plane was considered. A constant albedo value of 0.3 was used for its calculation.

Direct, diffuse and reflected irradiance were determined for each hour of the year. The sum of the three components allows obtaining the global irradiance at each hour of the year. The annual

global irradiance results from the integration of the global irradiances received during the year on each pixel.

4.5. Generation of the estimated solar thermal production map

For the development of the solar thermal production estimation map, it must be considered that the irradiance (G_T) incident on the surface of a thermal panel (A_{cap}), produces a useful thermal power at the collector output ($\dot{Q}_{cap}$) that can be determined from Eq. (5).

$$\dot{Q}_{cap} = \eta A_{cap} G_T. \tag{5}$$

This thermal power is used to heat the fluid flowing through the panel from its inlet temperature (T_i) to its outlet temperature (T_o), according to Eq. (6).

$$\dot{Q}_{cap} = \dot{m}_{cap} c_p (T_o - T_i), \tag{6}$$

where $\dot{m}_{cap}$ is the mass flow rate (density of the fluid multiplied by its volumetric flow rate) and c_p is the specific heat at constant pressure of the fluid.

The efficiency of the solar thermal panel (η) is not constant. For its determination, the Eq. (7) was used, which considers the data usually given by the solar panel manufacturers η_0, a_1 and a_2). This equation is a simplification of the one indicated for the stationary test method for liquid heating collectors in the UNE-EN ISO 9806 standard [19], where $T_m = (T_i - T_o)/2$.

$$\eta = \eta_0 - a_1 \frac{T_m - T_a}{G_T} - a_2 \frac{(T_m - T_a)^2}{G_T}. \tag{7}$$

Combining Eqs. (5) and (7), Eq. (8) is obtained, which allows, once defined the value of T_m, and the parameters η_0, a_1 and a_2 of the panel, obtaining the useful heat at the collector output from the irradiance data provided by the solar radiation map and the ambient temperature data. For the calculation of the useful thermal power, a value for the T_m of 50ºC was considered, and values of 0.813 for η_0, 3.674 for a_1 and 0.019 for a_2.

$$\dot{Q}_{cap} = \left[\eta_0 - a_1 \frac{T_m - T_a}{G_T} - a_2 \frac{(T_m - T_a)^2}{G_T}\right] A_{cap} G_T. \tag{8}$$

In addition, a thermal production density threshold was set below which the pixel in question is not considered useful for carrying out a solar thermal installation. This threshold was set at 70% of that corresponding to the best orientation and inclination with no obstacles in Pamplona. Together with the pixels that do not exceed such limit, those located less than 1 meter from the facades of the buildings were discarded for reasons related to installation and maintenance. This way it was generated the pixel-based solar thermal production map. It should be noted that the calculation of the thermal potential was performed for panels with the slope and orientation of the roofs of the buildings. That is, for flat roofs, the thermal potential was calculated on the horizontal plane. Therefore, an optimization of the position of the thermal panels was not addressed in this work.

4.6. Estimation of the solar thermal potential of the roof of each rooftop

From the map obtained through the methodology described in Section 4.5, we proceeded to the aggregation of pixel information by building and by ZIP code using QGIS software. For this purpose, the cadastral information of Pamplona was used.

5. Results and discussion

The value of the global solar radiation received annually at each pixel of the DSM can be seen in Figure 3, and Figure 4 shows a detail of the above map for two areas of the city.

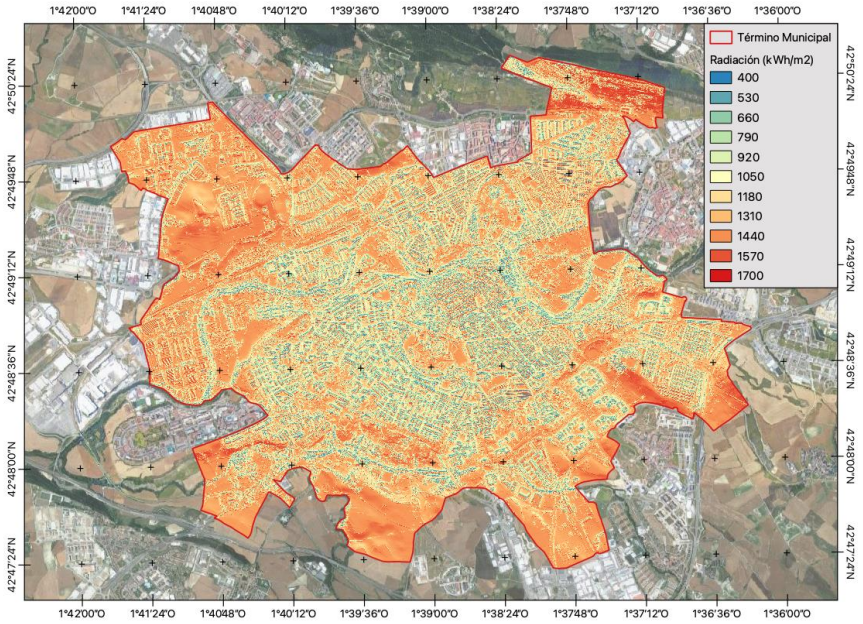

Figure 3. Annual global solar radiation map.

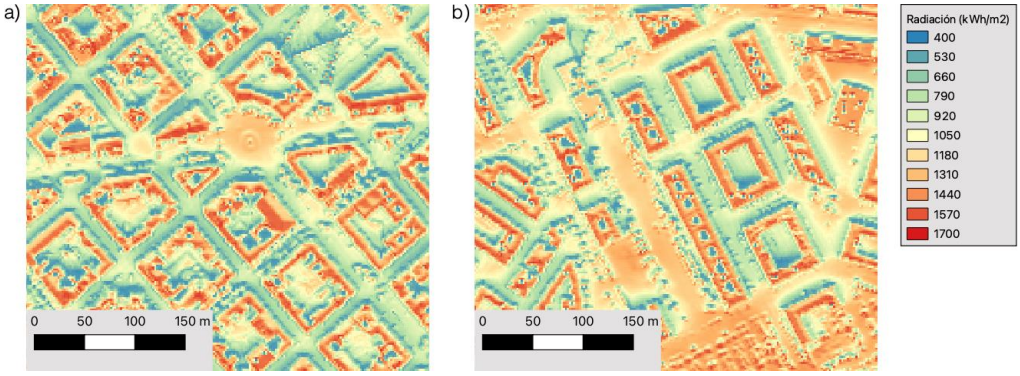

Figure 4. Detail of the annual global solar radiation map in two areas of Pamplona: Segundo Ensanche (a) and Rochapea (b).

Figure 5 shows the thermal energy density (kWh/m^2) obtained after the simulation of the considered thermal system, whereas Figure 6 shows a detail of the above map for two areas of the city.

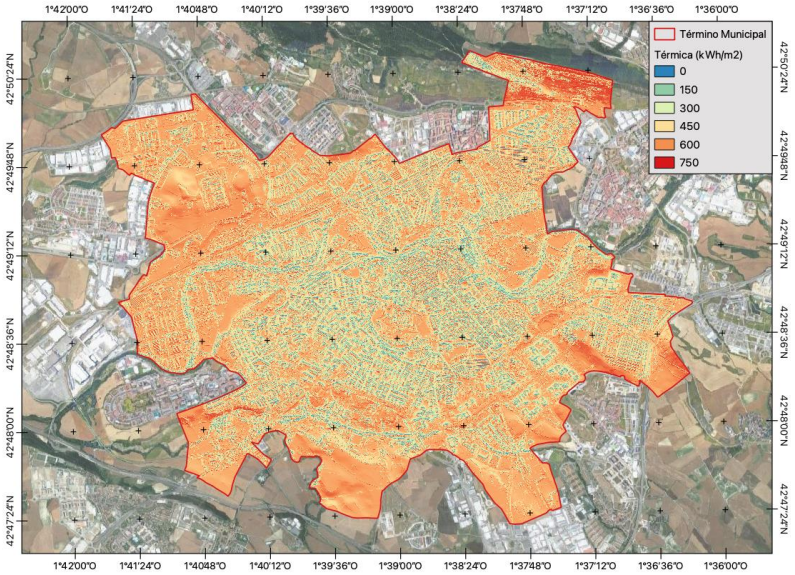

Figure 5. Map of annual output thermal energy densities per pixel.

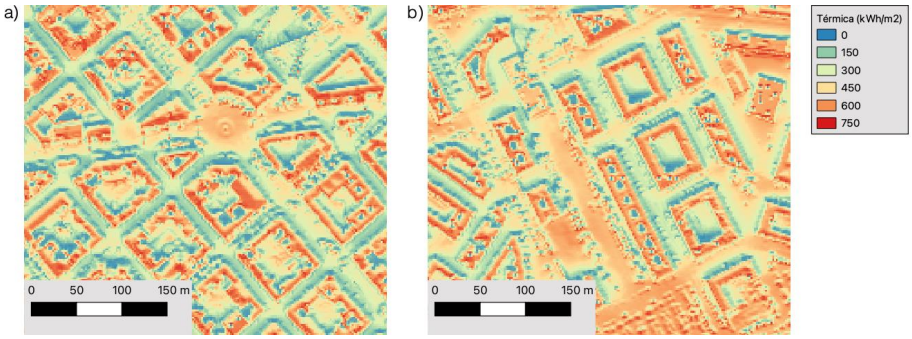

Figure 6. Detail of the map of annual thermal energy output densities per pixel in two areas of Pamplona: Segundo Ensanche (a) and Rochapea (b).

The values of thermal energy density obtained after applying the criterion of tilt and misalignment losses and 1 meter setback with respect to the facade line can be seen in Figure 7. Here, the areas shaded in gray are not suitable for solar thermal energy utilization.

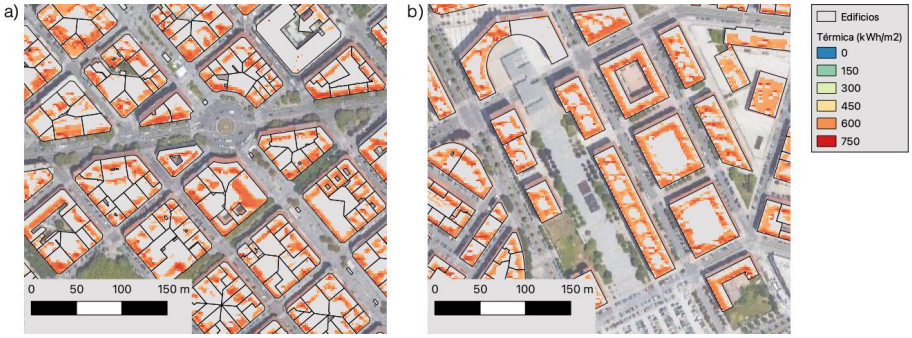

Figure 7. Detail of the annual thermal energy output densities of suitable pixels in two areas of Pamplona: Segundo Ensanche (a) and Rochapea (b).

Figure 8 shows a detailed map of annual thermal production (kWh) per building.

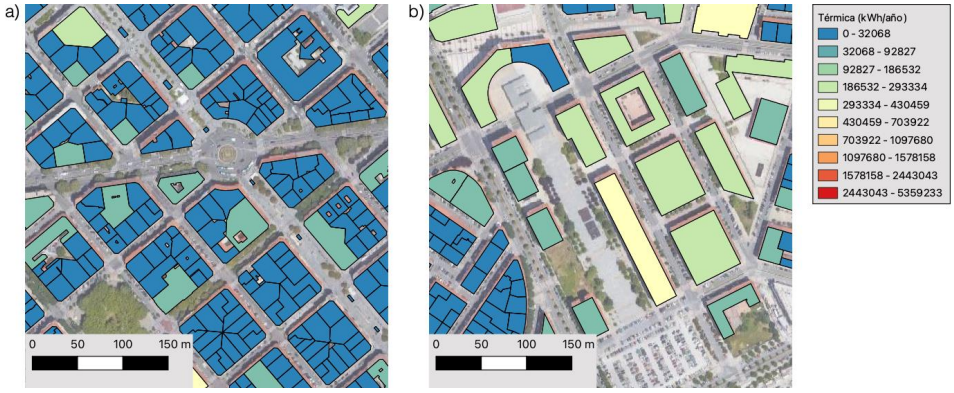

Figure 8. Detail of the map of annual thermal productions by buildings in two areas of Pamplona: Segundo Ensanche (a) and Rochapea (b).

After aggregating the solar thermal production potential per building (see Fig. 8), the overall values for the whole city were obtained. Figure 9 represents the total possible solar thermal production of Pamplona for each month of the year, according to the thermal map. This results in a total annual solar thermal energy production of 1197.69 GWh. If renewable solar energy supply and demand were perfectly coupled over time, it would be possible to achieve an annual thermal demand coverage of 99.1%, considering a total annual natural gas consumption of 1208 GWh. However, in many cases, the highest thermal energy consumption does not coincide with the times when solar radiation and, therefore, solar thermal production are highest. Unfortunately, the information on monthly thermal consumption in Pamplona was not available, so it was not possible to perform a monthly analysis of the rates of coverage of thermal demand by solar energy.

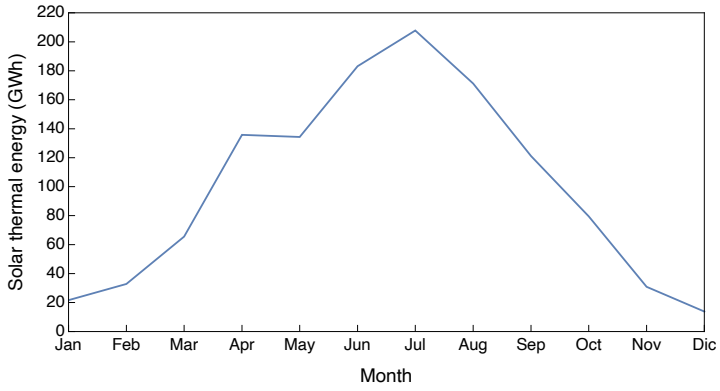

Figure 9. Monthly solar thermal production in the city of Pamplona.

Figure 10 shows the annual thermal production values by postal district. The postal district 31012, which concentrates most of the city's industrial fabric, stands out for its high solar thermal energy production potential (233.98 GWh).

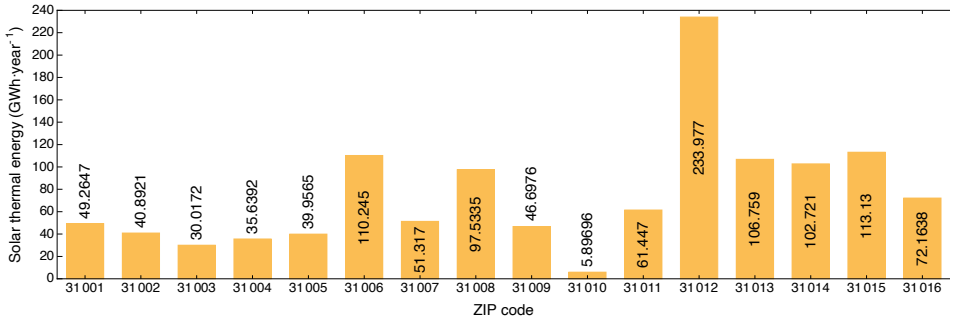

Figure 10. Annual solar thermal production for the postal districts of the city of Pamplona.

6. Conclusions

The solar map of the city of Pamplona and, specifically, the solar thermal energy production map presented in this study constitutes a fundamental tool for energy planning in the city and a stimulus for the implementation of individual solar thermal installations. This detailed map allowed estimating a total solar thermal energy production potential for the whole city of 1197.69 GWh. All the information generated in this work can be consulted through the municipal geographic viewer of the City Council of Pamplona, through the following link: https://www.pamplona.es/agenciaenergetica/mapasolar.

Solar thermal potential estimates were obtained for the current inclination and orientation of the roof surfaces of the buildings. A possible future line of work could focus on determining the optimal arrangement of thermal panels installed on the available flat roofs and estimating their solar thermal potential.

Acknowledgements

The authors gratefully acknowledge the financial support provided by the Government of Navarre. Ignacio García thanks to the Spanish Ministry of Universities and the European Union-Next Generation EU for their financial support (Program for the requalification of the Spanish university system 2021-2023, Resolution 1402/2021).

References

[1] United Nations, The World's Cities in 2018—Data Booklet (ST/ESA/ SER.A/417), 2018.
[2] United Nations, The Paris Agreement, 2015. [Online]. Available: https://unfccc.int/process-and-meetings/the-paris-agreement/the-paris-agreement.
[3] European Comission, A European Green Deal, 2019. [Online]. Available: https://ec.europa.eu/info/strategy/priorities-2019-2024/european-green-deal_en#documents.
[4] A. Verso, A. Martin, J. Amador, and J. Dominguez, GIS-based method to evaluate the photovoltaic potential in the urban environments: The particular case of Miraflores de la Sierra, *Sol. Energy*, vol. 117, pp. 236–245, Jul. 2015.
[5] G. Agugiaro, F. Nex, F. Remondino, R. De Filippi, S. Droghetti, and C. Furlanello, SOLAR RADIATION ESTIMATION ON BUILDING ROOFS AND WEB-BASED SOLAR CADASTRE, *ISPRS Ann. Photogramm. Remote Sens. Spat. Inf. Sci.*, vol. I–2, pp. 177–182, Jul. 2012.
[6] T. Gómez-Navarro, T. Brazzini, D. Alfonso-Solar, and C. Vargas-Salgado, Analysis of the potential for PV rooftop prosumer production: Technical, economic and environmental assessment for the city of Valencia (Spain), *Renew. Energy*, vol. 174, pp. 372–381, Aug. 2021.

[7] C. N. Long and E. G. Dutton, BSRN Global Network Recommended QC Tests, v2.0, in *Report No 1-3*, 2002.
[8] I. García and J. L. Torres, Temporal downscaling of test reference years: Effects on the long-term evaluation of photovoltaic systems, *Renew. Energy*, vol. 122, pp. 392–405, Jul. 2018.
[9] R. Perez, P. Ineichen, E. L. Maxwell, R. Seals, and A. Zelenka, Dynamic global to direct conversion models, *ASHRAE Trans. Res. Ser.*, pp. 354–369, 1992.
[10] J. L. Torres, M. De Blas, A. García, and A. de Francisco, Comparative study of various models in estimating hourly diffuse solar irradiance, *Renew. Energy*, vol. 35, no. 6, pp. 1325–1332, Jun. 2010.
[11] M. de Blas, J. L. Torres, J. Polo, and J. M. Vindel, Aplicación de los modelos DirInt y DirIndex para estimar la irradiancia solar directa a partir de irradiancia global en Pamplona (Navarra), in *Actas del VII Congreso Ibérico de Agroingeniería y Ciencias Hortícolas*, 2013.
[12] M. Dirksen, G. Pagani, R. Ronda, and N. Theeuwes, Sky view factor calculations and its application in urban heat island studies, *Urban Clim.*, vol. 30, 2019.
[13] K. Lee and G. Levermore, Sky view factor and sunshine factor of urban geometry for urban heat island and renewable energy, *Archit. Sci. Rev.*, vol. 62, no. 1, 2019.
[14] J. Böhner and O. Antonić, *Geomorphometry - Concepts, Software, Applications*, vol. 33, no. C. Elsevier, 2009.
[15] J. Dozier and J. Frew, Rapid calculation of terrain parameters for radiation modeling from digital elevation data, *IEEE Trans. Geosci. Remote Sens.*, vol. 28, no. 5, pp. 963–969, 1990.
[16] M. J. Blanco, K. Milidonis, and A. M. Bonanos,Updating the PSA sun position algorithm," *Sol. Energy*, vol. 212, pp. 339–341, Dec. 2020.
[17] R. Perez, P. Ineichen, R. Seals, J. J. Michalsky, and R. Stewart, Modeling daylight availability and irradiance components from direct and global irradiance, *Sol. Energy*, vol. 44, no. 5, pp. 271–289, Jan. 1990.
[18] I. García, J. L. Torres, M. de Blas, C. Sáenz, B. Hernández, and R. Illanes Muñoz, Evaluación comparativa de 19 modelos de estimación de irradiancia difusa sobre planos inclinados dependiendo del tipo de cielo estándar ISO/CIE, in *As Energias Renováveis na Transição Energética: Livro de Comunicações do XVII Congresso Ibérico e XIII Congresso Ibero-americano de Energia Solar*, 2020, pp. 869–877.
[19] AENOR, Norma Espanola UNE-EN-ISO 9806. Energía Solar. Captadores Solares Térmicos, Métodos de Ensayo, p. 130, 2020.